Kinetics of Strain Aging in Bake Hardening Ultra Low Carbon Steel—a Comparison with Low Carbon Steel

A.K. De, S. Vandeputte, and B.C. De Cooman

(Submitted 22 February 2000)

The kinetics of the static strain aging process have been analyzed in a vacuum-degassed ultra low carbon bake hardenable (ULC BH) steel with a total carbon content of 20 wt.ppm through measurement of the strength properties. The influence of prestrain and free interstitial carbon content has been studied. The kinetic results were compared with those of a BH low carbon (LC) steel. In the derivation of the time exponent and the activation energy, only the first stage of aging was considered. It was observed that, at all prestrain levels and matrix solute carbon contents, the initial aging process in the ULC steel obeyed the $t^{2/3}$ kinetic law and the kinetics were not influenced by the changes in dislocation structure due to prestrain and the dissolved carbon content. In comparison, the aging process and the kinetics in the LC steel were found to be significantly influenced by the amount of prestrain. The presence of carbide particles in LC steels can modify the aging kinetics.

Keywords internal friction, kinetics, LC BH steel, prestrain, strain aging, ULC BH steel

1. Introduction

Bake hardenable (BH) vacuum-degassed ultra low carbon (ULC) steels (C < 50 wt.ppm) have recently received increased attention for autobody applications in the automotive industry. Compared to low carbon (LC) BH steels (C > 100 wt.ppm), ULC BH steels have excellent forming properties and an increased strength that is achieved due to the aging during the paint baking of the final product. These steels can be processed on hot dip galvanizing/galvannealing lines without an overaging section, which is necessary for LC steels to allow cementite precipitation. Bake hardening is essentially a strain aging process resulting from the interaction between interstitial carbon atoms dissolved in the matrix and the dislocations generated during forming operation. The kinetics of the process is controlled by the long-range diffusion of interstitial atoms to the strain fields of dislocations. Atmospheres of interstitial atoms are formed in the vicinity of the dislocation cores. Further segregation of interstitials to the dislocations results in carbide precipitation. The most obvious manifestation of the strain aging process is the increase in the yield stress of the material at all solute levels and aging times.[1] Earlier investigations of the strain aging process in Fe-C alloys have established distinctly the mechanisms and stages of the process.[2–4] With regard to the kinetics of the aging process, it is likely that the entire aging process cannot be described by a single model. The initial stage of the aging process was originally described by Cottrell and Bilby's kinetic model.[5] According to Cottrell and Bilby, during the atmosphere formation, the total number of solute atoms n_t segregating to per unit length of dislocation in time t is given by

$$n_t = n_0 3\left(\frac{\pi}{2}\right)^{\frac{1}{3}}\left(\frac{ADt}{kT}\right)^{\frac{2}{3}} \qquad \text{(Eq 1)}$$

where n_0 is the number of solute atoms per unit volume, A is the interaction energy between a dislocation and solute atom, and D is the diffusion coefficient of the segregating solute at the absolute temperature T. With the advance of the aging process, Eq 1 fails, however, to describe the kinetics, as it does not consider the solute depletion surrounding the dislocations, a fact which was also recognized by Cottrell.

In order to extend the applicability of the model to systems of supersaturated Fe-C solid solutions, Harper modified the above equation to allow for the lowering of solute concentration in the matrix surrounding the dislocations as the aging proceeds.[6] He assumed that the rate of segregation at any time would be proportional to the solute concentration remaining in solution and obtained

$$W = \frac{n_t}{n_0} = 1 - \exp\left[-3L\left(\frac{\pi}{2}\right)^{\frac{1}{3}}\left(\frac{ADt}{kT}\right)^{\frac{2}{3}}\right] \qquad \text{(Eq 2)}$$

where W is the fraction of solute atoms already segregated in time t and L is the total length of dislocations per unit volume. Harper found a good agreement with his experiments for fractions of solute depletion up to 0.90. The limitations to the Harper model have been reviewed by Baird.[7] As the Harper model does not allow for the back diffusion from the core of dislocations, it can only be valid for steels with low atmosphere densities. In many strain aging studies in the Fe-C system, a generalized form of Harper's equation has been used to derive the kinetics of the aging process. Equation 2 can be rewritten as

$$\ln(1 - W) = -\left(\frac{t}{\tau}\right)^n = -(kt)^n \qquad \text{(Eq 3)}$$

A.K. De and **B.C. De Cooman,** Laboratory for Iron and Steelmaking, Ghent University, 9052 Ghent, Belgium; and **S. Vandeputte,** OCAS N.V., Research Centre of the SIDMAR Group, 9060 Zelzate, Belgium. Contact e-mail: bruno.decooman@rug.ac.be.

where τ is a temperature-dependent relaxation constant obeying an Arrhenius-type relation from which the activation enthalpy of the aging process can be derived. The kinetic parameters n and ΔH derived from fitting experimental data to Eq 3 have often been used to interpret precipitation mechanisms or to take into account dislocation inhomogeneities. Any deviation in the value of n from $^2/_3$ is generally regarded as being associated with a change in the precipitation mechanism of carbon on dislocations or in the matrix.[8–12]

In BH ULC steel, a very low amount of carbon is retained in solid solution at the end of processing and the precipitation of iron carbides is unlikely to take place in this type of steel.[13] Moreover, because of the ultra low level of solute content, the C backdiffusion is expected to be insignificant. Therefore, the application of the Harper derivation should give an accurate description of the aging kinetics until the completion of the atmosphere formation in ULC steels.

Strain aging in ULC BH steel is technologically very important. Presently, attempts are being made to increase the bake hardenability of these steels through retention of more solute carbon in the matrix by increasing the cooling rates after soaking in a continuous annealing cycle. In this work, the strain aging results of a BH ULC steel have been examined with respect to changes in prestrain and solute carbon content resulting from the application of different cooling rates after annealing. The kinetic parameters n and ΔH of the aging process were determined with the analytical models describing atmosphere formation. The influence of the prestrain and the solute carbon content on the time exponent n was evaluated. In the derivation of the kinetics, the increase in upper yield strength due to the aging process was taken into account rather than the solute segregation, as the former is the most consistent manifestation of the atmosphere formation process. This consideration also stems from the fact that a very small amount of carbon is required for atmosphere formation even for a highly deformed material. Considering the occupancy of one carbon atom per atomic plane threaded by the dislocation at atmosphere saturation, the amount of carbon required to saturate a dislocation density of ρ (m^{-2}) in bcc ferrite can be calculated as

$$[\mathrm{C}]_{\mathrm{ppm}} = 8.9 \cdot 10^{-15} \cdot \rho \qquad \text{(Eq 4)}$$

So, even for a large dislocation density of $10^{14}/\mathrm{m}^2$, only about 1 ppm carbon is needed to saturate all the dislocations. Whereas in the past the C aging has been successfully analyzed by means of internal friction (IF) or resistivity measurements, no diagnostic tool is presently available to monitor accurately such extremely low levels of carbon segregation during atmosphere formation.

2. Application of Kinetic Models

2.1 Harper Model

From Eq 3, a plot of ln [−ln (1 − W)] against ln t will result in a straight line with a slope n and a y intersect proportional to the diffusivity of the interstitial solute. Since k is expressed as $k = k_0 \exp[-(\Delta H/RT)]$, a plot of ln k versus $1/T$ will give the activation energy of the aging process.

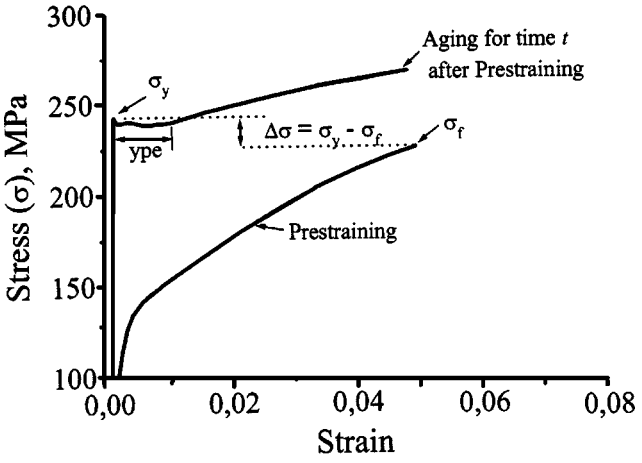

Fig. 1 Measurement of increase in yield stress $\Delta\sigma$ due to strain aging

The parameter W has often been equated to the fractional increase in yield stress, $\Delta\sigma/\Delta\sigma_{max}$, during the aging process, where $\Delta\sigma$ is the increase in yield stress after aging for time t and $\Delta\sigma_{max}$ is the maximum stress increment due to prolonged aging.[1] The proportionality between W and $\Delta\sigma/\Delta\sigma_{max}$ may be questioned when the aging process occurs in supersaturated solid solutions, where the strengthening may result from different concurrent mechanisms, but it probably is a fair approximation in the case of the ULC steels.

2.2 Hartley Model

This is the only model available so far that allows the kinetics of strain aging to be derived by measuring the changes in yield stress. Hartley described the increase in yield stress during aging as due only to the reduction of mobile dislocation length, which is proportional to the linear concentration of carbon on the dislocations. Hartley proposed the following aging kinetic equation:[14]

$$\frac{(\sigma_y - \sigma_f)}{^1/_2(\sigma_y + \sigma_f)} = \frac{\Delta\sigma}{\overline{\sigma}} = K_1 + K_2\left(\frac{Dt}{T}\right)^{2/3} \qquad \text{(Eq 5)}$$

where σ_y is the upper yield stress after prestraining and aging, σ_f is the flow stress at the end of prestraining (Fig. 1), t is the aging time, T is the aging temperature, D is the diffusion coefficient,[14] and K_1 and K_2 are constants for constant test conditions, The slope S of the $\Delta\sigma/\overline{\sigma}$ versus $t^{2/3}$ plot is given by $S = K_2 (D/T)^{2/3}$. With $D = D_0 \exp[-(\Delta H/RT)]$, the activation energy ΔH for carbon diffusion therefore can be easily obtained from the plot of ln ($ST^{2/3}$) versus $1/T$.

However, apart from dimensionality consideration, the physical interpretation of the use of the term $^1/_2(\sigma_y + \sigma_f)$ is not clear in Hartley's derivation.[14] Since in the derivation of Eq 5 the degree of atmosphere saturation has been taken into account instead of the total fraction of solute segregating to the dislocations, it was considered more appropriate to use the term $\Delta\sigma/\Delta\sigma_{atm}$ for the degree of saturation in the present work, where $\Delta\sigma_{atm}$ is the maximum increase in yield stress at atmosphere saturation. It has been observed that the maximum

Table 1 Chemical composition of the steels (in wt.%)

Steel	C	Mn	P	S	Al	Ti	N
ULC	0.0020	0.09	0.045	0.0030	0.0490	0.0070	0.0016
LC	0.039	0.18	0.035	0.0070	0.0540	…	0.0044

increase in yield stress $\Delta\sigma_{atm}$ at atmosphere saturation is constant for a prestrain level up to 10% and aging temperatures up to 170°C for the ULC steel investigated.[13]

Therefore, from Eq 5, if the time exponent is set as n, then the slope of the ln $\Delta\sigma/\Delta\sigma_{atm}$ versus ln t plot will give the value of n.

3. Experimental Procedure and Material

3.1 Material and Processing

The material used for the present study was a vacuum-degassed ULC BH steel with the composition as given in Table 1. The aging results for a LC BH steel with the composition given in Table 1 were used to compare the kinetics of aging.[15]

The hot-rolled sheets of both the ULC and LC steel were given 75% cold reduction in a laboratory cold rolling mill. After cold rolling, the sheets were annealed in a (Carl-Wezel, Germany) continuous annealing simulator at 850 °C for 60 s with an overaging cycle of 180 s at 400 °C. The cooling rate from the annealing temperature was 10 °C/s. The annealed sheets were further given a temper rolling reduction of 1.3%.

Tensile specimens of 80 mm gage length were prepared from these sheets and were prestrained 2, 5, and 10% at a strain rate of 4×10^{-4} s^{-1} and then aged at temperatures between 50 and 170 °C for different times in a silicone oil bath with a temperature control of ±1.5 °C.

For varying the amount of solute carbon content in the matrix of the ULC steel, the cold-rolled sheets were cooled from the annealing temperature of 850 °C at three different cooling rates: (1) sheets cooled at the rate of 10 °C·s^{-1}, (2) sheets cooled at the rate of 50 °C·s^{-1} to room temperature, and (3) sheets water quenched from the annealing temperature at the rate of 550 °C·s^{-1} to room temperature. In the review of the aging results, these samples are designated as (a) SC (slow cooling, 10 °C·s^{-1}), (b) MC (medium cooling, 50 °C·s^{-1}), and (c) FC (fast cooling, 550 °C·s^{-1}). Tensile specimens prepared from these sheets were prestrained 5% and then aged at 50 °C for different times.

3.2 Mechanical Testing

The increase in yield stress $\Delta\sigma$ was determined as the difference between the upper yield stress, σ_y, after aging for time t and the flow stress, σ_f, at the end of prestraining based on the original specimen dimensions (Fig. 1).

The solute carbon content in the SC, MC, and FC specimens was determined by IF measurements using a high frequency piezoelectric ultrasonic composite oscillator. In this technique, the specimen is set to vibrate longitudinally over a piezoelectric oscillator at 40 kHz at a vibration strain amplitude of 10^{-7}. The IF due to stress-induced ordering of interstitials is recorded during the fast heating (100 °C/min) of the specimen in an infrared radiator furnace over a temperature range of 20 to 300 °C.[16] At 40 kHz, the Snoek peak occurs at around 192 °C. The inherent advantage associated with this technique is that it has a very high signal-to-noise ratio compared to the conventional torsion pendulum instrument. Hence, a very low amount of interstitials can be traced accurately with this instrument. An additional advantage of this technique is that, as the interstitial carbon segregates to the dislocations during heating to the peak temperature, one measures the actual interstitial C content in the matrix at the paint baking temperature.

4. Results and Discussion

4.1 Aging Behavior—ULC and LC Steel and Effect of Prestrain

Figures 2(a) and (c) describe the aging behavior in the prestrained ULC steel with respect to time and temperature. It is observed that, at all prestrain levels, the increase in strength reaches a distinct saturation plateau after a time characteristic of the aging temperature. The strength then remains almost constant during further aging. Except for a marginal increase in strength in specimens prestrained 2% at higher aging temperatures, no second stage of hardening, *i.e.*, carbide precipitation, can be seen. This suggests that the solute carbon available in the matrix of the ULC steel (SC sheets) is sufficient only to complete atmosphere formation. The attainment of the saturation plateau marks the end of Cottrell atmosphere formation, as studied previously through the changes in yield point elongation (YPE) behavior.[13] Second, at all prestrain levels and temperatures of aging, the maximum strength increase at the end of the atmosphere formation, $\Delta\sigma_{atm}$, was found to be ≈30 MPa.

In comparison, the aging in the LC steel has two distinct stages (Fig. 2d and e). A significant strength increase is observed in the second stage or the precipitation stage in the LC steel. The maximum increase in strength decreases with the increase in prestrain.

4.2 Effect of Cooling Rate

Figure 3 shows the IF spectra observed for the SC, MC, and FC specimens due to different rates of cooling. The carbon content in the matrix increases with the increase in cooling rate, as reflected in the IF spectra. The solute carbon content in the rapidly cooled specimens will be slightly higher than what is measured considering the 2 min heating time needed to reach the peak temperature of measurement. Rapid cooling introduces some dislocations or vacancies in the material, and, hence, there is a possibility of losing some interstitial carbon to the dislocations during the measurement. This effect is expected to be very limited in slowly cooled specimens (Eq 4).

The strain aging results of these specimens for an aging temperature of 50 °C are shown in Fig. 4(a) and (b) with respect to changes in yield stress and YPE. The distinct features revealed in the aging results are as follows.

- With increasing interstitial carbon content, the aging stage now gradually advances to the second stage of aging and

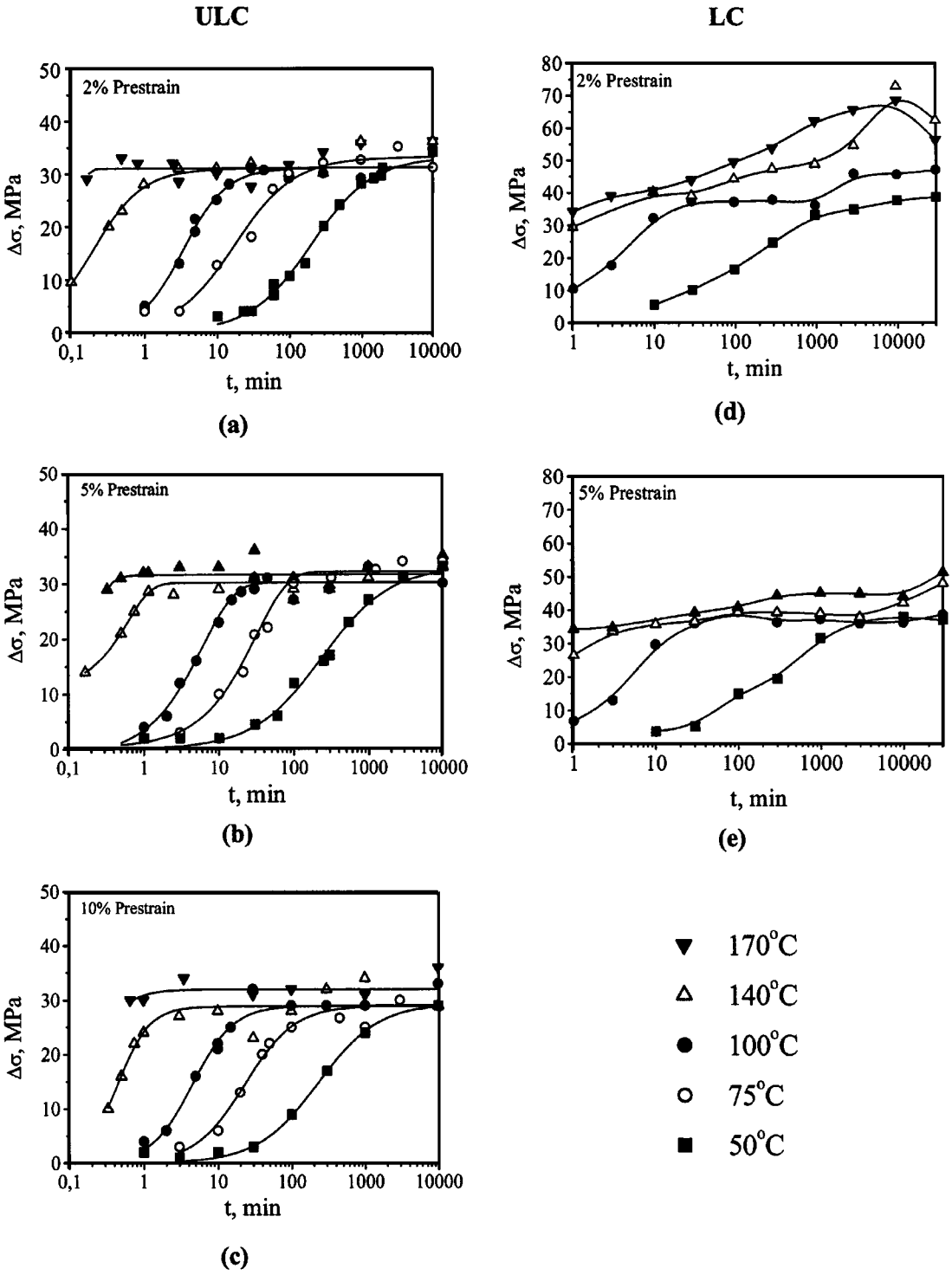

Fig. 2 Increase in the yield stress with time for different aging temperatures for prestrained (**a**) to (**c**) ULC and (**d**) and (**e**) LC steels

a significant second stage hardening is observed in the FC and MC specimens.

- The completion of the first stage of aging or the atmosphere saturation occurs faster with the increase in carbon content, as revealed in the YPE results (Fig. 4b).
- The maximum increase in yield stress $\Delta\sigma_{atm}$ at atmosphere saturation (as indicated by the maximum in the YPE values) is again 30 MPa in all the SC, MC, and FC specimens.

4.3 Kinetics of Aging

The aging results of Fig. 2(a) to (c) were replotted in terms of Eq 3 and 5 and are shown in Fig. 5(a) and (b), respectively.

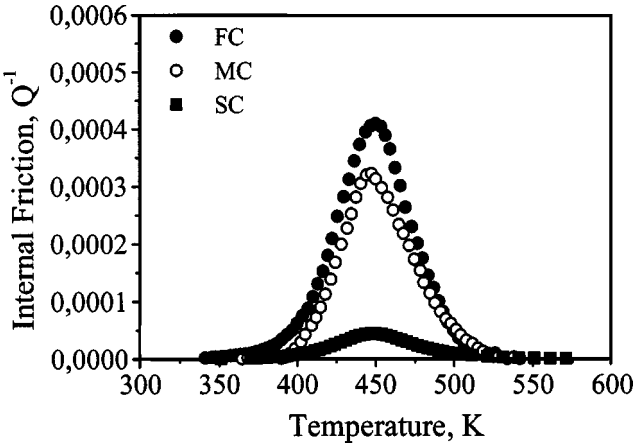

Fig. 3 IF spectra in annealed ULC specimens cooled at different rates

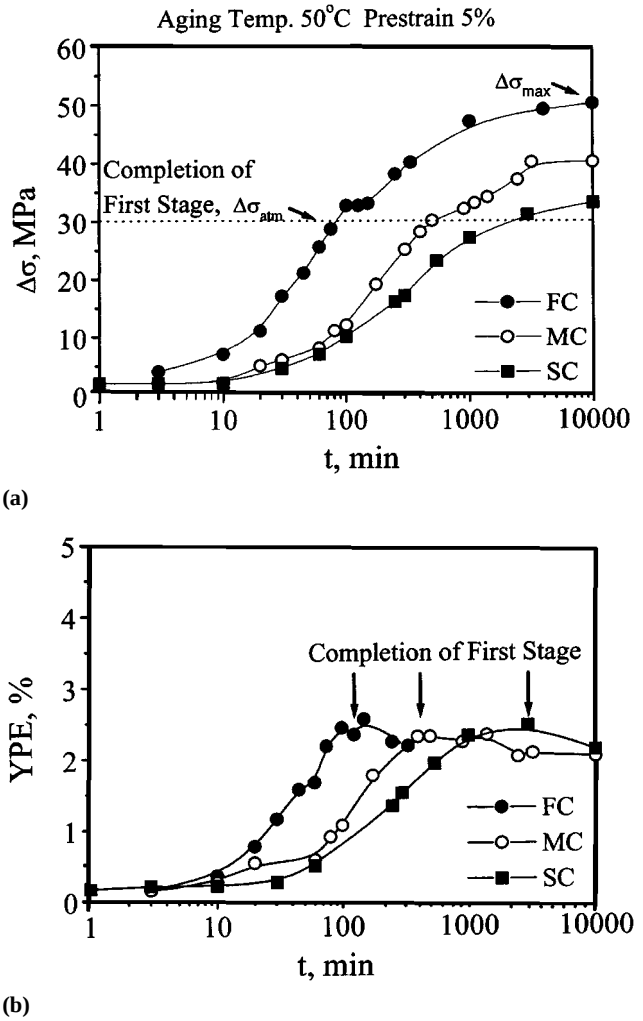

Fig. 4 Aging behavior in ULC specimens with different cooling rates with respect to (**a**) increase in yield stress and (**b**) YPE

Both the equations describe the data quite well up to the completion of atmosphere saturation at all the prestrain and temperature levels. The slopes *n* of these plots are tabulated in Table 2. It is clear from the figures that within the prestrain and temperature range studied, no change in the slopes is observed. The values of *n* found through Harrier's analysis fall within 0.65 to 0.80, which are quite close to that derived by Cottrell and Bilby for the interaction of the dislocation and the interstitial carbon for which $n \cong 0.66$. Values of *n* found through Hartley analysis are also close to the value of 0.66. However, relatively higher values obtained through Harper's model were due to the neglect of saturation effects in this model.

The analysis of the kinetics through these models suggests a normal strain aging kinetics ($t^{2/3}$ law), *i.e.*, carbon segregation to dislocations alone, and that the kinetics is not altered by the changes in the dislocation density in the ULC steels within the range studied. This is important since amplitude-dependent IF measurements on prestrained specimens demonstrated that prestraining the ULC steel in excess of 7.5% results in dislocation structure changes.[17] The TEM observation of thin foils of 10% prestrained specimens revealed the presence of cellular dislocation network formation. While the kinetics changes due to such dislocation structure changes have not been reported so far, but based on Bullough and Newman's analysis, a time exponent value of 0.77 had been reported earlier[18] considering inhomogeneities in dislocation distribution (in the region of clusters, cell walls, and carbides).

The aging results of the LC steel were also analyzed through the Harper and Hartley models for comparison of aging kinetics with those of ULC steel, and the results are shown in Fig. 6(a) and (b), respectively. The *n* values calculated from the data are given in Table 2. It is clear that in this case the amount of prestrain influences the values of *n* within the temperature range examined. The values of *n* for specimens prestrained 2% derived through the Harper (0.54 to 0.55) and Hartley (0.46 to 0.48) models are both lower than those observed for the ULC specimens. The results point more toward a $t^{1/2}$ kinetic law. In specimens prestrained 5%, the *n* values are much closer to the Cottrell's $t^{2/3}$ law. In other words, at higher prestrain, the Cottrell atmosphere formation process dominates, whereas at lower prestrain, the *n* values are suggestive of a mechanism of carbon diffusion toward a growing cementite particle. In a recent work by Kozeschnik and Buchmayr,[19] it was shown that within a prestrain range of 0 to 5% there is a change in the precipitation mechanism. They indicated that, at low dislocation density, the precipitation of carbide is favored and, at about 5% prestrain and more, the ferrite matrix is depleted by Cottrell atmosphere formation and no carbide particles can form until at least the majority of carbon atoms have diffused to the dislocations. In earlier works,[11] a $t^{1/2}$ kinetic law had been found to be associated with dislocation locking by carbon atoms at ferrite-cementite interfaces. The LC steel contains many cementite particles[15] and also a higher amount of manganese than the ULC steel. Therefore, it is likely that the carbide particles can grow during aging and lead to an additional increase in yield stress.[8,20] Leslie[8] demonstrated that, during aging of an Fe-Mn-C alloy at temperatures between 60 and 100 °C, precipitation of carbides both in the matrix and the dislocations could be observed as Mn shortens the incubation time

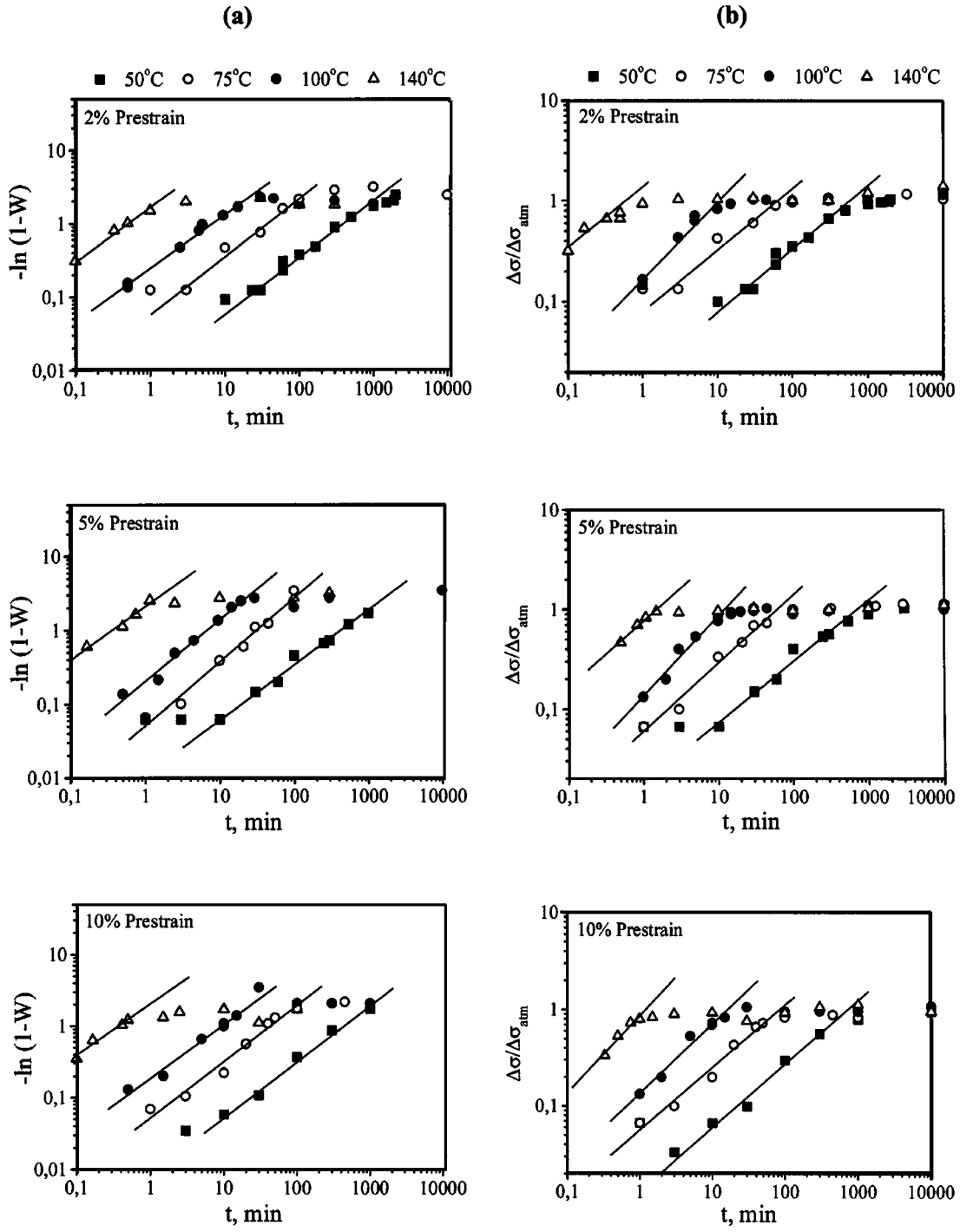

Fig. 5 Kinetic analysis of the aging data of prestrained ULC specimens using (**a**) Harper and (**b**) Hartley models

for the formation of critical nuclei and affects the activity of carbon.

The analysis of the aging data for specimens with different solute carbon contents (Fig. 4) is given in Fig. 7(a) and (b). The values of *n* measured from the slopes of these plots are given in Table 3. It is interesting to note that the slopes are almost constant for all the specimen groups and are very close to the value of 0.66. This suggests that, even with changing the solute carbon content (within 20 wt.ppm), the aging mechanism does not change. Earlier aging results with higher initial carbon content reported abrupt changes in aging kinetics in quenched-in iron alloys which were ascribed to the changes in aging mechanism from nucleation on dislocation only to the nucleation within the matrix and dislocations.[8,9] The nucleation within the matrix is said to be facilitated by the presence of vacancy rings generated due to quenching.[8] This

Table 2 Kinetic parameters *n* and Δ*H* for the strain aging process in the ULC and LC steels as a function of prestrain and temperature

Steel	Model	Prestrain, %	Aging temperature, °C	*n*	Δ*H*, kcal/mol
ULC	Harper	2	140	0.69	19.6
			100	0.70	
			75	0.76	
			50	0.75	
		5	140	0.65	20.0
			100	0.65	
			75	0.80	
			50	0.72	
		10	140	0.73	20.3
			100	0.74	
			75	0.78	
			50	0.73	
	Hartley	2	140	0.59	19.0
			100	0.76	
			75	0.61	
			50	0.63	
		5	140	0.65	19.0
			100	0.79	
			75	0.68	
			50	0.61	
		10	140	0.80	19.7
			100	0.71	
			75	0.64	
			50	0.66	
LC	Harper	2	50	0.55	15.7
			100	0.54	
		5	50	0.67	19.2
			100	0.80	
	Hartley	2	50	0.46	16.8
			100	0.48	
		5	50	0.64	21.8
			100	0.58	

was expected in the present case for FC specimens, but the present results suggest that, even if such a mechanism is present, it does not influence the aging process strongly. This is probably due to the fact that even the highest solute carbon in the FC specimen is too low to cause any matrix nucleation.

The activation energy for the atmosphere formation process in ULC steel was calculated from Fig. 5(a) and (b) using both Harper and Hartley derivations, and the results are shown in Fig. 8(a) and (b), respectively, for the two models. The values are given in Table 2 and are in excellent agreement with the activation energies of 18 to 20.1 kcal/mol for diffusion of carbon in bcc iron during strain aging, as published earlier.[6,21] The activation energies derived for the LC steel specimens apparently show a strong prestrain dependence. At higher prestrain, the activation energy derived (Table 2) is close to that for diffusion of carbon atoms to the dislocations, whereas at lower prestrain, a much lower activation energy is found. This implies that the underlying aging mechanism in the LC steel is not the same at all prestrains, a fact that was also revealed in the *n* values (Table 2).

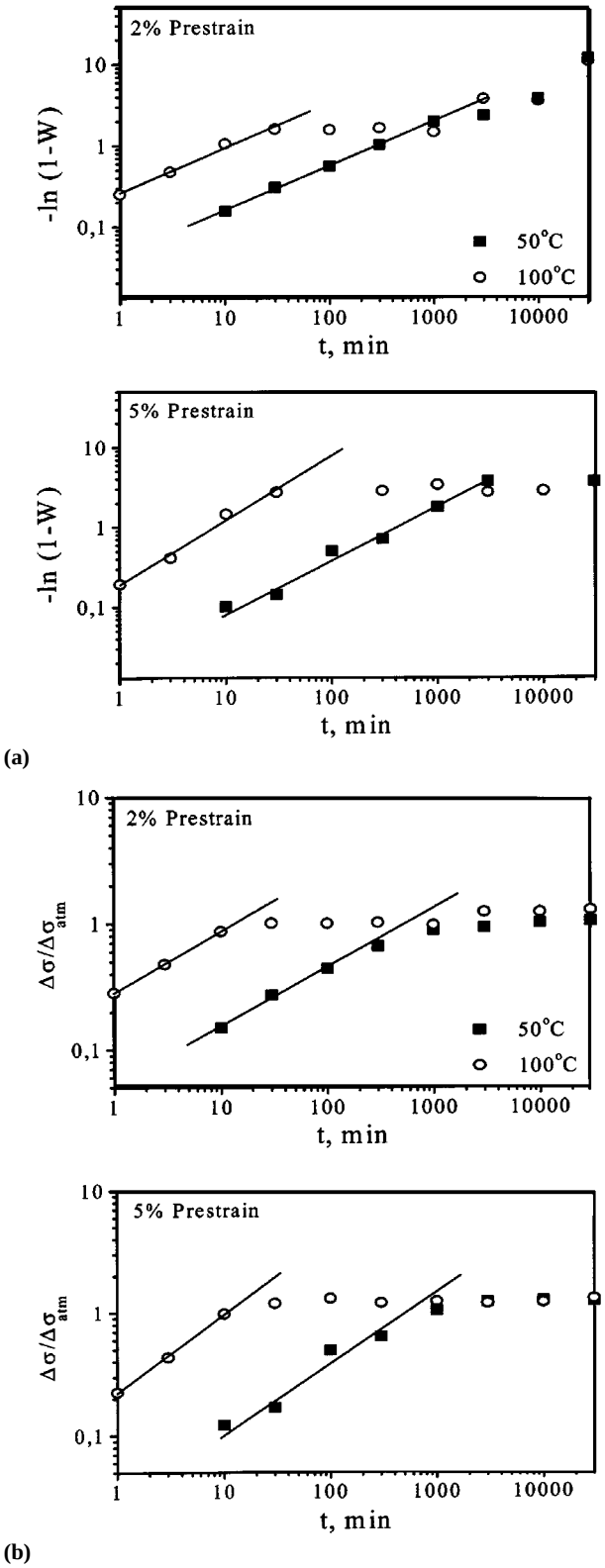

Fig. 6 Kinetic analysis of the aging data for prestrained LC specimens using (**a**) Harper and (**b**) Hartley models

5. Conclusions

In the present work, an attempt was made to apply the available analytical models describing kinetics of strain aging to the aging results of an ULC and a LC steel, in order to compare the aging kinetics for these steels and to obtain the

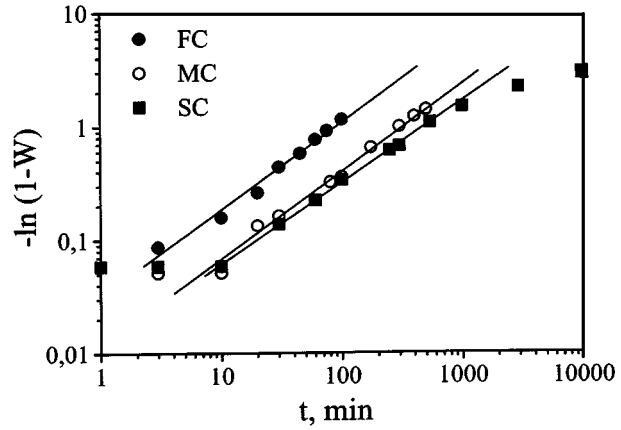

(a)

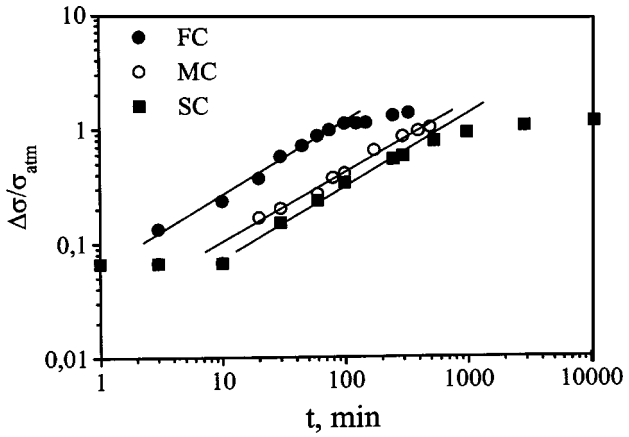

(b)

Fig. 7 Kinetic analysis of the aging data of SC, MC, and FC specimens using (**a**) Harper and (**b**) Hartley models

Table 3 Kinetic parameter *n* for the strain aging process in the ULC steel as a function of cooling rate

Model	Prestrain, %	Aging temperature, °C	Cooling rate	*n*
Hartley	5	50	10 °C·s^{-1}	0.63
			50 °C·s^{-1}	0.60
			550 °C·s^{-1}	0.63
Harper	5	50	10 °C·s^{-1}	0.71
			50 °C·s^{-1}	0.76
			550 °C·s^{-1}	0.76

kinetic parameters *n* and ΔH. The kinetics were derived through measurement of the increase in yield stress due to aging. The following conclusions can be drawn.

- The time exponent *n* evaluated through different kinetic models suggested that the dislocation pinning by the carbon atoms is the dominant mechanism during the strain aging in the ULC BH steel at all prestrain levels and is not affected by the changes in dislocation structure due to straining.
- The amount of prestrain up to 10% or the changes in solute carbon content (up to 20 wt.ppm) does not influence the aging kinetics in the ULC steel.

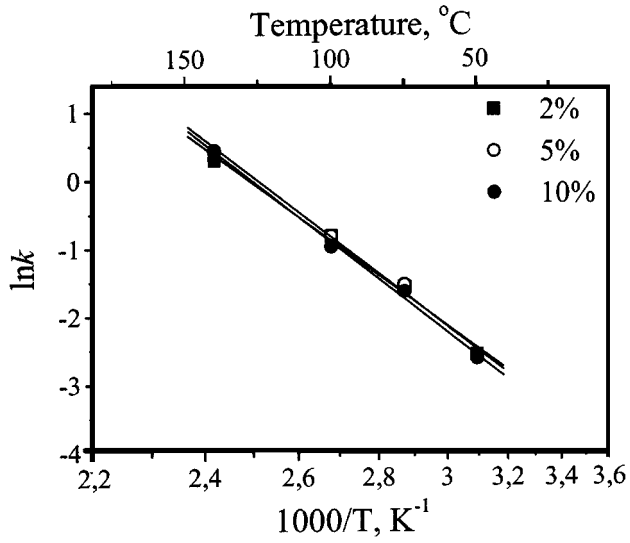

(a)

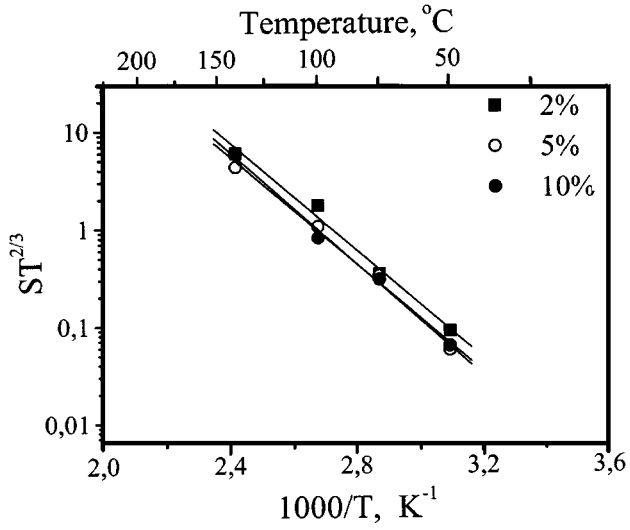

(b)

Fig. 8 Determination of the activation energy of carbon diffusion during strain aging in prestrained ULC specimens using (**a**) Harper and (**b**) Hartley model

- The maximum increase in yield stress at atmosphere saturation is 30 MPa in the ULC steel, and this does not depend on the amount of prestrain or solute content within the range studied.
- The activation energy for the atmosphere formation stage in the ULC steel has been found to be 19 to 20.3 kcal/mol, which is in excellent agreement to the activation energy of 18 to 20.1 kcal/mol for diffusion of carbon in bcc iron during strain aging reported previously in the literature.

In the case of the LC BH steel, the dislocation density has a significant role in determining both the strengthening level after the second stage of aging and the kinetics of the initial aging process. At lower prestrain, the kinetics follows a $t^{1/2}$ law, and at higher prestrain, the kinetics is governed mainly by

the dislocation and carbon atom interaction, which follows a $t^{2/3}$ time dependence.

References

1. W.C. Leslie: *The Physical Metallurgy of Steels,* McGraw-Hill, New York, NY, 1982, p. 88.
2. W. Pitsch and K. Lücke: *Arch. Eisenhüttenwes.,* 1956, vol. 1, p. 45.
3. D.V. Wilson and B. Russell: *Acta Metall.,* 1960, vol. 8, pp. 36-45.
4. P. Elsen and H.P. Hougardy: *Steel Res.,* 1993, vol. 64, pp. 431-36.
5. A.H. Cottrell and B.A. Bilby: *Proc. Phys. Soc.,* 1949, vol. A62, pp. 49-62.
6. S. Harper: *Phys. Rev.,* 1951, vol. 83, pp. 709-12.
7. J.D. Baird: *Iron and Steel,* 1963, vol. 7, pp. 368-74.
8. W.C. Leslie: *Acta Metall.,* 1961, vol. 9, pp. 1004-22.
9. R.H. Doremus: *Trans. AIME,* 1960, vol. 218, pp. 596-605.
10. S.I. Neife, E. Pink, and H.P. Stüwe: *Scripta Metall. Mater.,* 1994, vol. 30, pp. 361-66.
11. V.T.L. Buono, M.S. Andrade, and B.M. Gonzalez: *Metall. Trans. A,* 1998, vol. 29A, pp. 1415-23.
12. R. Bullough and R.C. Newman: *Proc. R. Soc.,* 1959, vol. A249, pp. 427-40.
13. A.K. De, S Vandeputte, and B.C. De Cooman: *Scripta Mater.,* 1999, vol. 41, pp. 831-37.
14. S. Hartley: *Acta Metall.,* 1966, vol. 14, pp. 1237-46.
15. A.V. Snick, K. Lips, S. Vandeputte, BC De Cooman, and J. Dilewijns: in *Proc. on Processing and Properties,* W. Bleck, ed., Aachen, Germany, 1998, Modern LC and ULC Sheet Metals for Cold Forming, vol. 2, pp. 413-24.
16. I.G. Ritchie and Z. Pan: *33rd MWSP Conf. Proc.,* ISS, Warrendale, PA, 1992, vol. 29, pp. 15-25.
17. A.K. De, K. De Blauwe, S. Vandeputte, and B.C. De Cooman: *J. Alloys Compounds,* 2000, vol. 310 (1–2), pp. 405-10.
18. J.D. Baird: *Iron and Steel,* 1963, vol. 8, pp. 400-05.
19. E. Kozeschnik and B. Buchmayr: *Steel Res.,* 1997, vol. 68 (5), pp. 224-30.
20. T. Obara, K. Sakata, M. Nishida, and T. Irie: *Kawasaki Steel Technical Report,* 1985, vol. 12, p.25.
21. C. Wert: *Phys. Rev.,* 1950, vol. 79, pp. 601-05.